Composites: Part B 58 (2014) 328–334

Contents lists available at ScienceDirect

Composites: Part B

journal homepage: www.elsevier.com/locate/compositesb

Resin infusion analysis of nanoclay filled glass fiber laminates

K. Kanny *, T.P. Mohan

Composites Research Group, Department of Mechanical Engineering, Durban University of Technology, Durban, South Africa

ARTICLE INFO

Article history:
Received 28 June 2012
Received in revised form 13 September 2013
Accepted 25 October 2013
Available online 7 November 2013

Keywords:
A. Hybrid
A. Laminates
B. Rheological properties
E. Thermosetting resin
Nanoclay

ABSTRACT

This paper focuses on the resin flow characteristics of nanoclay filled glass fiber laminates processed by Vacuum Assisted Resin Infusion Molding (VARIM). Laminates with varying quantities of nanoclays (0–5 wt.%) were prepared and the effect of these nanoclays on the epoxy resin flow characteristics was studied. It was found that the flow rate of resin continuously decreased as nanoclay content continuously increased. The reduction in the flow rate was attributed to the rate of change of curing and the subsequent change in viscosity of the nanoclay filled resin. Analysis of infusion process by Darcy's law show that the permeability of the fiber decreased in the nanoclay filled resin system. Nanoclay filled laminates show improved static and dynamic mechanical properties than that of unfilled resin composites.

1. Introduction

Glass fiber reinforced composites are an important class of material due to their high strength to weight ratio when compared to steel, and their high corrosion and chemical resistance [1–3]. These composite laminates also consist of a range of fibers such as carbon, Kevlar and glass. They are widely used in aircraft, transportation, civil and other engineering applications [4–6].

Over the past two decades, a considerable amount of research work has been done on polymer–clay nanocomposites (PCN). Chemically treated nanolayered montmorillonite (MMT) based clays are widely used as nanofillers in these PCN based structures [7–11]. The addition of small amount of treated MMT clay (~5 wt.%) in epoxy and other polymer matrices has caused dramatic improvement in mechanical, thermal, physical and chemical properties [12–16].

The nanoparticle filled polymer reinforced with glass fibers has also been an area of research interest in past 5–7 years. In this type of composite structure, the glass fibers serve as a primary reinforcement and nanoparticles as secondary reinforcement. In such structures, the nanoparticles such as clays, carbon nanotubes, and nanosilica/TiO2 are filled in the laminate and are processed either by hand lay up, vacuum assisted infusion, hot-press or other forming techniques [17–21]. The nanoparticle infused laminates have shown improved thermal and mechanical properties [22–24] and improved fiber–matrix interface strength [25]. The study of nanoclay filled epoxy based laminate composite is a complex subject. The dispersion of clay particles in a polymer is governed by the mixing process, catalytic curing of organo-ions, the curing agent and the processing method [26–29]. From literature it is observed that the effect of clays on laminate processing is not yet fully understood. Therefore in this work we have studied the effect of clay on the processing parameters and the subsequent mechanical properties of nanoclay filled epoxy polymer reinforced with woven glass fiber. The laminates were processed using Vacuum Assisted Resin Infusion Molding (VARIM). The authors' view is that the results of this study will help the designers to control the processing properties of the laminates, namely thickness, fiber volume fraction (V_f), degree of cure (α), permeation, structure and morphology of nanoclay reinforced laminates.

2. Experimental details

2.1. Raw materials

In this study, diglycidyl ether of bisphenol-A (DGEBA) based commercial epoxy resin supplied under the trade name of LR-20 was used as the matrix. The curing agent was unmodified cyclic aliphatic amine based epoxy hardener supplied under the trade name of LH-281. Silane treated E type plain weave glass woven roving (450 GSM) was used as the primary reinforcement. All these materials were purchased from AMT Composites, Durban – South Africa. The secondary nanoclay reinforcement filler, supplied under the trade name Cloisite-30B, was purchased from Southern Clay Products, Inc., USA. Cloisite 30B is an organically modified MMT clay with MT2EtOH based Tallow compound, where MT2EtOH is

* Corresponding author. Tel.: +27 031 373 2230; fax: +27 031 373 2139.
E-mail address: kannyk@dut.ac.za (K. Kanny).

1359-8368/$ - see front matter © 2013 Elsevier Ltd. All rights reserved.
http://dx.doi.org/10.1016/j.compositesb.2013.10.025

methyl tallow bis-2-hydroxyethyl quaternary ammonium compound.

2.2. Laminate preparation

Glass fiber reinforced and nanoclay filled epoxy hybrid laminates were prepared by Vacuum Assisted Resin Infusion Molding (VARIM) process. The processing of laminates involved two steps: the first step was mixing of nanoclays in the epoxy resin and the second step was the infusion of the modified resin into the glass fiber rovings.

Six (6) layers of plain weave glass fiber (WGF) rovings were cut to size 35 cm × 35 cm, and subsequently weighed. An equivalent weight of epoxy resin to that of the 6 layers of WGF was used. Nanoclays of various weight percentages (0–5 wt.%) to that of epoxy/hardener mixture was taken and mixed with epoxy resin at room temperature. The mixing was carried out for 1 h at 500 rpm with mechanical stirrer. After mixing the resin with the clay 30 wt.% of hardener (equivalent to epoxy resin weight) was added to the epoxy-clay mixture and then processed to form a laminate. The laminates were processed by using a vacuum pressure of 0.5–2 bars. During the resin infusion process, the time taken for the resin to flow to predetermined points was taken and the corresponding viscosity and degree of cure (α) was measured.

2.3. Characterization

The viscosity of the unfilled and nanoclay filled resin system was measured using a Brookfield viscometer according to the ASTM D2393-86 method. FTIR spectra of the epoxy, the clay, the glass fiber, the unfilled and the clay filled epoxy glass fiber hybrid composite was evaluated in the Attenuated Total Reflectance (ATR) mode, in the 800–4000 cm^{-1} range. FTIR spectroscopy was performed at the different stages of processing of composite laminate to evaluate degree of cure. The laminate was water quenched periodically during processing so as to ascertain the degree of cure (α) at a given time. The degree of cure was measured using FTIR, in which the ratio of peak value of epoxide oxirane group of cured to uncured samples was measured as discussed elsewhere [30]. Three samples were used to measure viscosity and obtain FTIR spectra, and the average values were considered for discussion.

The structure of the composites was examined using X-ray diffraction (XRD) and Transmission electron microscopy (TEM). A Philips PW1050 diffractometer was used to obtain the X-ray diffraction patterns using Cu Kα lines (λ = 1.5406 Å). The diffractrograms were scanned from 3° to 16° (2θ) in steps of 0.02° with a scanning rate of 0.5°/min. Microscopic investigation of selected specimens at the various weight compositions were conducted using a Philips CM120 transmission electron microscope with an operating voltage of 120 kV.

The fiber volume fraction was determined by polymer matrix burning method. In this method, a composite laminate of size 5 cm × 5 cm was cut, weighed and then burnt in a furnace at 800 °C. The unburnt fibers were weighed and the volume fraction of fibers was calculated.

Dynamic mechanical analysis was carried out at a frequency of 10 Hz in a 3-point bending mode using the TA instruments model Q800 from 25 °C to 130 °C at atmospheric conditions. Specimen of size 5.5 cm × 1 cm × 0.3 cm was used for this test.

Tensile test of composites was carried out at room temperature according to ASTM D 3039-08 method using MTS-UTM machine. For tensile test, a constant load of 1 kN and strain rate of 1 mm/min was kept and the tensile parameters (elongation to break, failure strength and stiffness) were measured. Five samples were cut from each composite panel and then tested. The mean values were considered for graphical representation and discussion.

3. Results and discussions

3.1. Flow characteristics

The flow characteristic of the resin and the resin-clay mixture was studied by measuring the time taken for the resin to flow across the laminate during processing. Fig. 1 shows the time vs distance curve of unfilled and nanoclay filled epoxy resin. The results indicate that unfilled resin flows faster than filled resin and the flow speed decreases with increase in nanoclay content. Flow speed of unfilled resin was 1.48 mm/s and this reduced to 0.9 mm/s for 5 wt.% nanoclay filled resin. In order to better understand this finding the viscosity and degree of cure (α) of filled and unfilled resin was studied further. Fig. 2 represents the viscosity of filled and unfilled resin at various points across the length of the laminate. A uniform viscosity of 4525 cP was observed in unfilled epoxy resin across the entire laminate length. The nanoclay filled resin system on the other hand displayed a distinct initial resin mixture viscosity (η_i) and a time dependent gel viscosity (η_g) and the viscosity of resin increased as the clay content increased. The viscosity of 5 wt.% filled nanoclay increased to 5153 cP (and 5322 η_g) from 4525 cP for unfilled laminate.

The viscosity was further examined by studying the curing characteristics of filled and unfilled resin. Fig. 3 shows the degree of cure of filled and unfilled resin at various stages of laminate processing. The results indicated that α remained unchanged in the unfilled laminate, but it continuously increased across the infusion length of the nanoclay filled laminate. The degree of cure for unfilled laminate was 6% and this increased to 21% in 5 wt.% nanoclay filled laminate. One possible reason for this increase may be due to the presence of organoions in the clay. Alkyl ammonium ions (organoions) of nanoclay may have catalyzed the curing of epoxy and hence increased the degree of cure. This is consistent with the finding reported elsewhere [31,32]. To gain an understanding of this phenomenon, a series of FTIR tests was performed. Fig. 4 shows the FTIR spectrum of unfilled and clay filled epoxies during processing. The characteristic peaks of unfilled epoxy resin were observed at 3467 cm^{-1} and 1630 cm^{-1} (peaks due to primary amines), 3000–2700 (CH stretching), 1514 cm^{-1} (aromatic ring), 1293 cm^{-1} (hydroxyl ether group) and 912 cm^{-1} (epoxide group) [33]. The characteristic peaks for the glass fiber was at 1120 cm^{-1} and 930 cm^{-1} due to Al_2O_3 and SiO stretching vibrations respectively [34]. Cloisite 30B showed the characteristic peaks at 1030 cm^{-1} Si–O plane stretching, 3440 cm^{-1} and

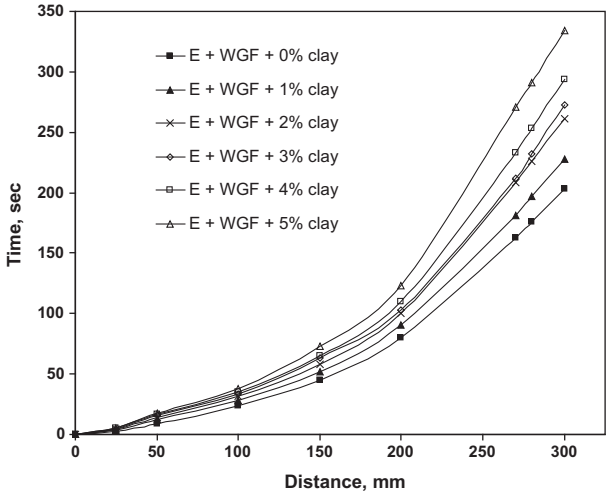

Fig. 1. Flow behavior of resin and resin-clay mixture during laminate processing.

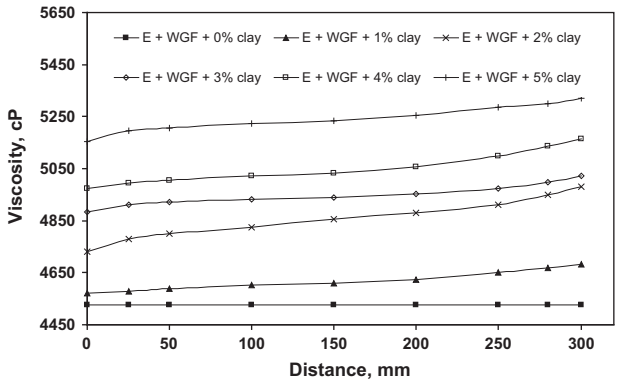

Fig. 2. Viscosity of epoxy and epoxy-clay mixture during laminate processing.

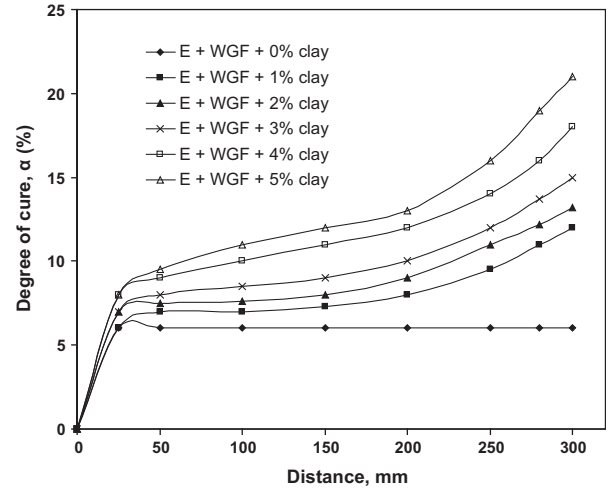

Fig. 3. Effect of clay content on the degree of cure (α) during laminate processing.

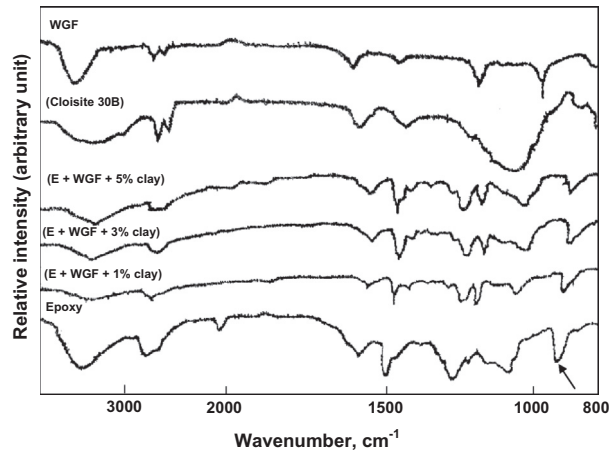

Fig. 4. FT-IR spectrum of partially cured epoxy, clay, glass fiber and epoxy-clay-glass fiber laminate mixture.

1630 cm^{-1} hydroxyl groups due to water molecules, 2929 cm^{-1}, 2846 cm^{-1}, 1437 cm^{-1} (organic C–H bands) [35]. FTIR spectrum of clay filled laminate showed the presence of all the constituents i.e., clay, epoxy and glass fiber and with reduced epoxide peak values at 912 cm^{-1} (this peak is indicated by an arrow, see Fig. 4). The reduction of epoxide peak was greater with corresponding increase in nanoclay content. The reduction of the epoxy peak suggests that the amine group acted as a catalyst during the epoxy curing and hence induce more favorable epoxy ring opening polymerization which resulted in increased degree of cure. This increased degree of cure possibly creates time dependent gel viscosity (η_g) [36,37]. Fig. 1 shows delayed resin infusion across the laminate due to increase in the degree of cure.

3.2. Compressibility

Fig. 5 shows the effect of vacuum on the laminate thickness as a function of clay content. The results suggested a reduction in laminate thickness (unfilled laminate) as the vacuum pressure increased. A 3.1 mm thick laminate reduced to 2.15 mm when vacuum pressure was changed from 0.5 bar to 2 bar. A similar effect was observed for nanoclay filled laminates; however, thickness reduction was much lower than the unfilled resin laminate. The rate of reduction of laminate thickness decreased as the nanoclay content increased. The thickness of 5 wt.% nanoclay filled laminate at 2 bar vacuum pressure was 3 mm. Due to the change in thickness of unfilled and clay filled laminates, the corresponding volume fraction (V_f) was also changed. Fig. 6 shows the effect of vacuum pressure on the fiber volume fraction. At 0.5 bar vacuum pressure the V_f of all the laminate series was approximately 0.46. The V_f of unfilled laminate increased as vacuum pressure increased, however, the rate of increase of V_f for filled resins reduced. At 2 bar vacuum pressure, the V_f was 0.62 and 0.47 for unfilled and 5 wt.% nanoclay filled laminate respectively. Amongst all the test samples, the lowest V_f change due to increased vacuum pressure was observed in 5 wt.% nanoclay filled laminate. This result suggests that the compressibility property of the nanoclay filled laminates was superior to unfilled laminates. These phenomena may be attributed to the increased viscosity of filled resin and the increased degree of cure.

The rheological property of resin flow front was studied by measuring the permeability of the glass fibers during resin infusion. Using Darcy's law as per Eq. (1), the permeability (k) was be calculated as,

$$Q = \frac{-kA}{\mu}\frac{(P_b - P_a)}{L} \tag{1}$$

where Q is the quantity of resin (g) that flows across the length L (mm) and with cross sectional area A (mm^2). μ is the viscosity of the resin (cP) at length L, P_a and P_b are the initial pressure and pressure at length L.

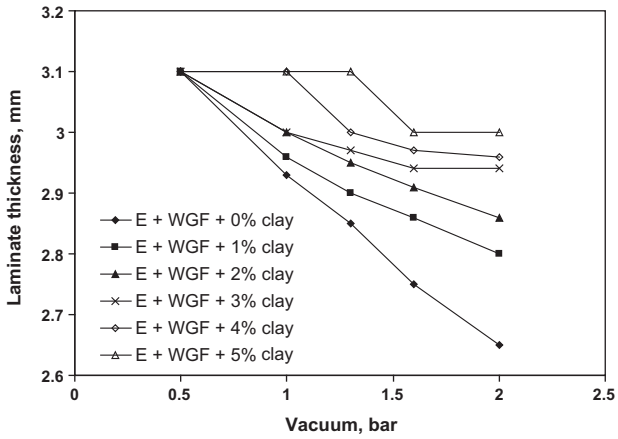

Fig. 5. Effect of vacuum on laminate thickness of composites.

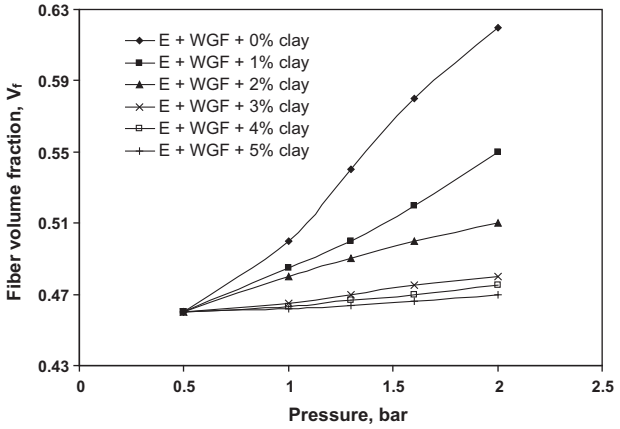

Fig. 6. Compressibility characteristics of laminates.

Fig. 7 shows the permeability (k) of the woven glass fiber using both filled and unfilled epoxy. The results show that the permeability of fibers set in unfilled resin remained constant at 1400 mm^2 during entire infusion period, whereas k decreased as nanoclay content increased. Conversely, the k value of filled resin reduced as resin infusion length increased. This reduction of k value in clay filled resin may be due to the increased viscosity, degree of cure or reduced flow rate, or a combination of these events. The permeability of 5 wt.% nanoclay filled resin was 919 mm^2 and 707 mm^2 at 0 mm and 300 mm respectively. Clearly, the selection of infusion points in nanoclay filled hybrid composites is a critical parameter and must be considered during laminate processing, to maintain desired permeability, thickness and V_f.

3.3. Structure

Both the unfilled and nanoclay filled composite laminates were examined by using XRD and TEM in order to verify rheological properties. Fig. 8 shows the XRD patterns of Cloisite 30B clay, glass fiber, unfilled and clay filled laminates. Cloisite 30B has a sharp diffraction peak at 2θ of 5.63° corresponding to interlayer spacing (d) of 18.1 Å. Both glass fiber and unfilled epoxy resin do not have any XRD peaks and this suggests the materials are amorphous. On the other hand, XRD of nanoclay filled resin composites show a range of peak patterns corresponding to the different wt.% of clays. Epoxies with up to 3 wt.% nanoclay shows no distinct XRD peak corresponding to the diffraction peak of Cloisite 30B. The absence of diffraction peak suggests that the nanoclays are randomly dispersed in the matrix. Such type of structure is generally referred

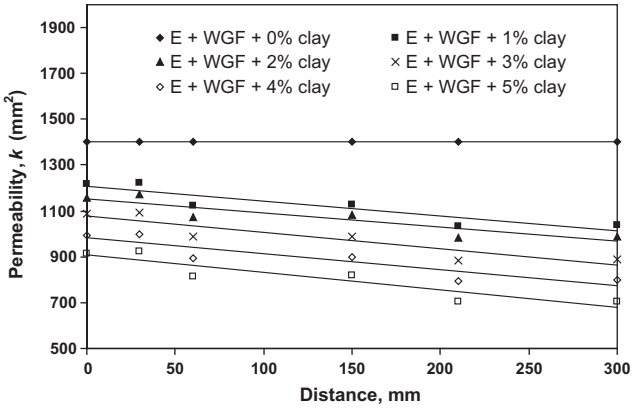

Fig. 7. Effect of clay on permeability (k) of fibers in a composite laminate.

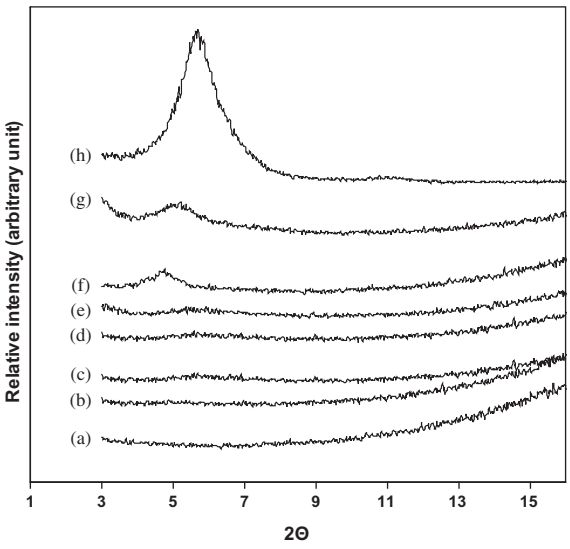

Fig. 8. XRD pattern of (a) glass fiber, (b) unfilled epoxy, epoxy with (c) 1% clay, (d) 2% clay, (e) 3% clay, (f) 4% clay, (g) 5% clay and (h) Cloisite 30B clay.

as an exfoliated nanocomposite structure [36]. Epoxies with 4 wt.% and 5 wt.% nanoclay show a sharp diffraction pattern at 2θ of 4.7° and 5.1° respectively, which corresponds to d-spacing of 23 Å and 21 Å respectively. The increased interlayer spacing suggests that the epoxy has intercalated into the gallery spacing of the clays. Such type of structures is referred to as an intercalated structure [36]. In the intercalated structure, the clay nanolayers are arranged in an orderly fashion in the matrix polymer and with increased interlayer distance compared to the clay itself. Here intercalated structure was observed only when the clay content was >3 wt.%. In order to better understand the morphology and distribution of nanoclay TEM studies were conducted. Fig. 9 shows the TEM of 1 wt.%, 3 wt.% and 5 wt.% nanoclay filled epoxy laminates where the bright phase is the matrix phase and the dark phase is the clay phase. TEM micrographs representing up to 3 wt.% clay filled laminate show the random arrangement of nanolayers in the polymer matrix confirming the exfoliated structure. TEM micrograph representing a 5 wt.% nanoclay filled epoxy laminate show the ordered arrangement of the nanolayers in the polymer matrix confirming the intercalated structure. TEM result supports the XRD result. Structural change occurred from exfoliation to intercalation as the function of clay content in epoxy polymer. As the clay content increased, the structure becomes intercalated structure, which could be related to rheological properties. Higher clay content had shown increased viscosity and catalyzed induced curing. The catalyzed curing might had resulted uneven curing at intergallergy region of clay and matrix region. Possibly the curing was faster in intergallery region than that of matrix region due to curing of organoions of clay with epoxy polymer. This effect could have restricted the clay nanolayer separation and also affected the random dispersion of nanolayers (exfoliated structure) in the epoxy polymer matrix, and resulted in intercalated structure for higher clay content.

3.4. Mechanical properties

Fig. 10 shows the tensile stress–strain curves for unfilled and the nanoclay filled laminate series, and the corresponding values are shown in Table 1. The results indicate that the addition of nanoclay has an effect on the tensile property of the laminate. Tensile strength, modulus and strain values increased with an increase in clay content. Similar findings are reported elsewhere [37–40].

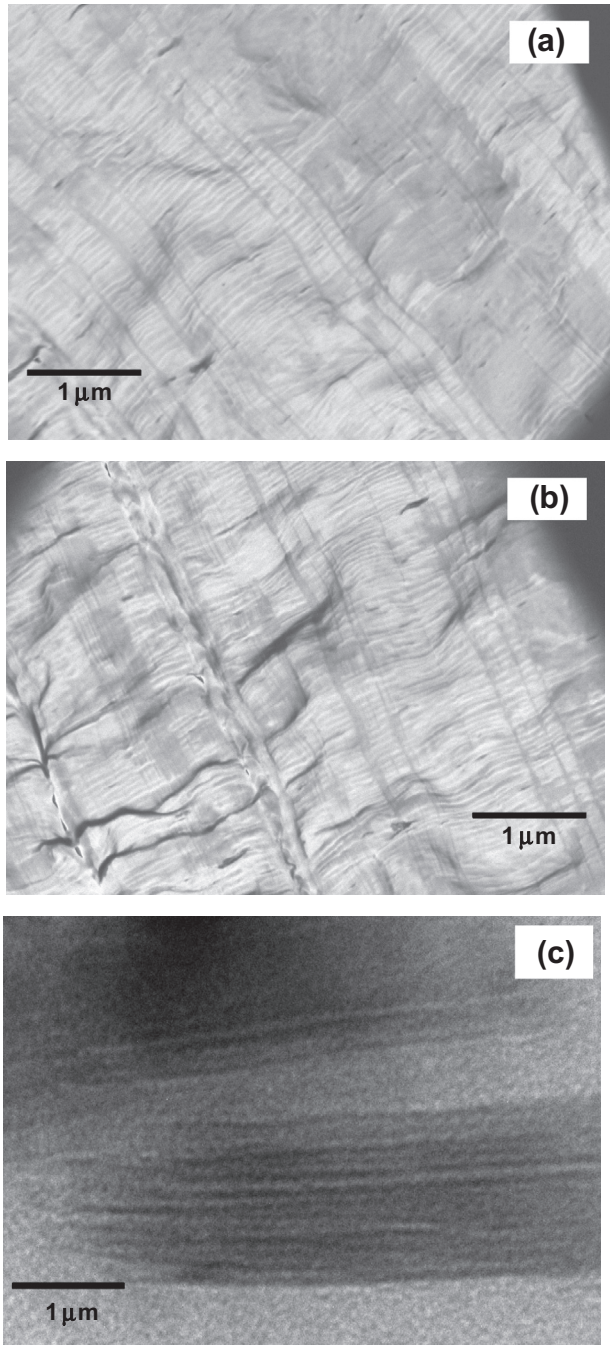

Fig. 9. TEM image of epoxy laminate with (a) 1 wt.% clay, (b) 3 wt.% clay and (b) 5 wt.% clay.

Reasons for improved tensile properties may be attributed to the high modulus of the clay and the improved deformation mechanisms once the nanoclay particles are infused in the polymer matrix. Fig. 10 shows the tensile stress–strain curves for all laminates, and an exploded view of the elastic portion of stress–strain curves is shown as an insert. Tensile properties (Table 1) shows continuous increase in properties up to 3 wt.% of nanoclay content. 3 wt.% nanoclay filled laminates show about 9% increase in strength, 21% increase in modulus and 15% increase in elongation at break values when compared with unfilled laminate. However, above 3 wt.% a reduction in tensile properties was observed. This reduction of properties could be possibly due to the structural changes in the laminates due to nanoclay addition. Both XRD and TEM confirm the formation of exfoliated and intercalated

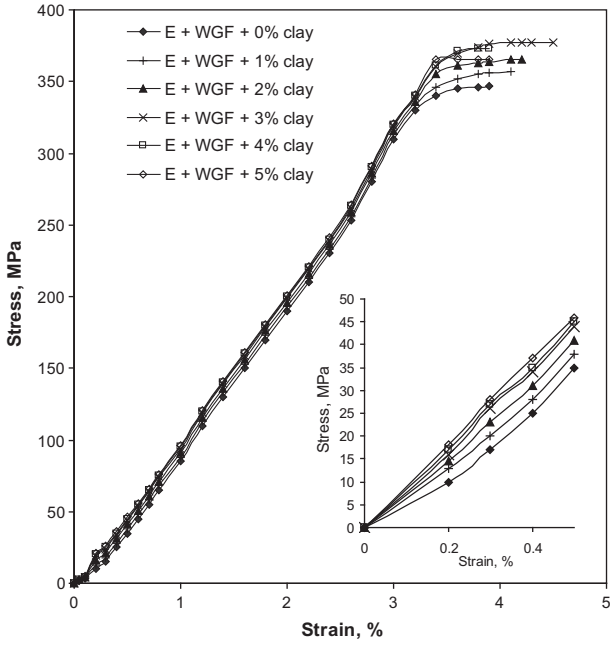

Fig. 10. Tensile stress–strain curves of laminate series.

structures. Literature results [41–45] suggest that the exfoliated structures have superior properties, perhaps because the aspect ratio of the clay nanolayer provide with increased surface contact area. Conversely, the morphology of an intercalated structure leads to the reduction in net aspect ratio of clay layer and surface contact area which results in inferior properties to that of an exfoliated structure. From the TEM micrograph (Fig. 9) we observe few of these factors, namely, segregation of nanolayers agglomerations or improper distribution of clay nanolayers in matrix material. These factors have reduced the tensile properties of laminates with greater than >3 wt.% clays.

Fig. 11 shows the dynamic mechanical analysis of nanoclay filled and unfilled laminate series and the corresponding values are shown in Table 2. The parameters of interest are storage modulus and glass transition temperature (T_g). The results indicate that the storage modulus is temperature dependent and reduced with a corresponding temperature increase. The temperature at which the maximum value of Tan δ observed in DMA test is the glass transition temperature of the polymer. The addition of clay affected the storage modulus and T_g of the laminates. Storage modulus and T_g continuously increased with an increase in nanoclay content up to 3 wt.%, after which a reduction of modulus and T_g occurred. Despite a reduction in storage modulus and T_g above 3 wt.%, the values were higher than that of unfilled laminates. Structural changes occurring in the material due to nanoclay content may be primary reasons for these changes. Nanoclays are hard phase material and has predominantly higher modulus (~167 GPa) [46] than that of epoxy polymer and glass fiber which have modulii of ~3.5 GPa and ~70 GPa respectively [47]. Similar improved storage modulus due to nanoclay addition was observed elsewhere [48]. The reduction of storage modulus above 3 wt.% could be linked to the formation of an intercalated nanocomposite structure. Table 2 shows that the T_g of the laminates increased in nanoclays. This is due to the thermal stability of nanoclays [48,49]. As the nanoclay content increased up to 3 wt.%, T_g of the polymer also increased. However, above 3 wt.%, T_g reduced, possibly due to the formation of an intercalated structure. In the intercalated structure, there is a lesser amount of polymeric surface exposed to the clay surface and this allows the polymer to deform due to heating, resulting in decreasing trend of T_g in laminates with above 3 wt.% nanoclays.

Table 1
Tensile properties of laminate series.

Material	Strength (MPa)		E-modulus (GPa)		Strain at break (%)	
	Mean	Std. Dev.	Mean	Std. Dev.	Mean	Std. Dev.
E + WGF	347	31	37	4	3.9	0.4
E + WGF + 1% clay	358	28	41	5	4.1	0.4
E + WGF + 2% clay	365	37	43	5	4.3	0.5
E + WGF + 3% clay	377	33	45	4	4.5	0.5
E + WGF + 4% clay	373	36	46	6	4.2	0.5
E + WGF + 5% clay	365	34	47	5	4.0	0.4

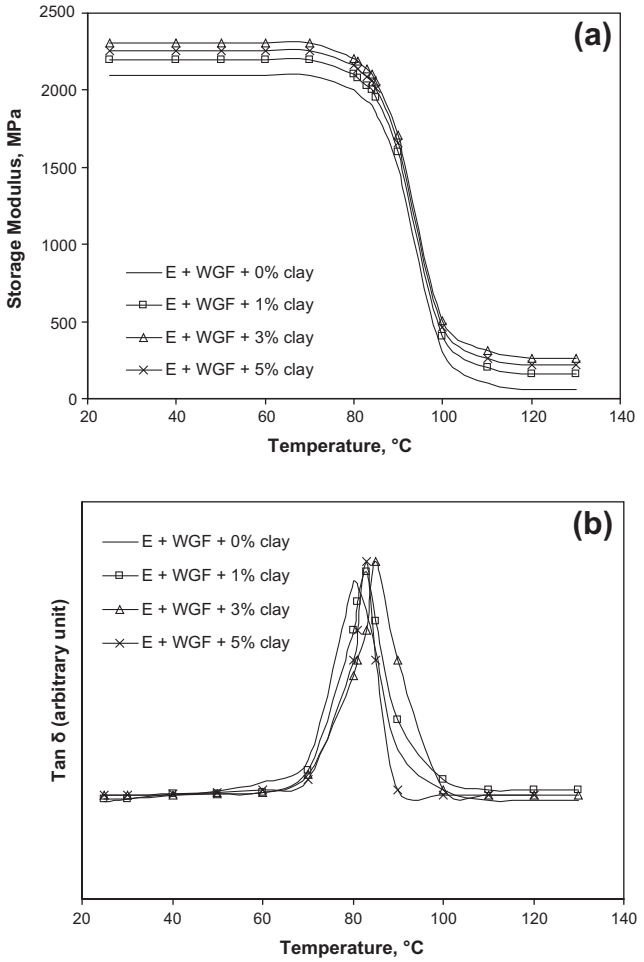

Fig. 11. Effect of temperature on (a) storage modulus and (b) Tan δ of laminate series.

Table 2
DMA properties of laminate series.

Material	Storage modulus at 25 °C (MPa)	T_g (°C)
E + WGF + 0% clay	2100	81
E + WGF + 1% clay	2201	83
E + WGF + 2% clay	2257	84
E + WGF + 3% clay	2308	86
E + WGF + 4% clay	2271	84
E + WGF + 5% clay	2260	83

4. Conclusions

A hybrid laminate composite comprising nanoclays, glass fiber and epoxy polymer was prepared using VARIM. The effect of nanoclay on rheology, compressibility, structure and mechanical properties of laminates was examined. The nanoclay content was varied from 0 wt.% to 5 wt.% in laminates. The result showed that the resin flow speed continuously decreased with corresponding increase of clay content. The flow speed for 5 wt.% nanoclay filled laminate was dropped to 0.9 m/s from 1.48 m/s which is for unfilled laminate. This change of resin flow speed in clay filled epoxy was due to the change in viscosity and degree of cure. Unfilled epoxy resin shows uniform viscosity across the entire laminate processing length. However, nanoclay filled resin shows two types of viscosities, namely, initial resin mixture viscosity (η_i) and time dependent gel viscosity (η_g). Both η_i and η_g values were continuously increased as nanoclay content continuously increased in resin. The η_i and η_g for 5 wt.% nanoclay filled resin was 5153 cP and 5322 cP respectively, while it was constant at 4525 cP in unfilled resin.

FTIR results indicated that the organoions of the clay act as catalyst during epoxy resin curing, and increased the degree of cure (α) and resulted in increased viscosity. The result also indicated that α remains unchanged across entire infusion period of unfilled resin, whereas it continuously increased across the infusion length as the nanoclay content increased in the laminate. Maximum improvement in α was observed in 5 wt.% nanoclay filled laminate. The α values are 6% and 21% for 0 wt.% and 5 wt.% nanoclay filled laminate.

The structural analysis (TEM and XRD) indicated that the nanocomposite formed exfoliated structure up to 3 wt.% nanoclay and above 3 wt.% formed intercalated structure. Due to the intercalated structure above 3 wt.% nanoclay, the material resulted in decreasing trend of tensile and DMA properties. Maximum improvement in these properties were observed at 3 wt.% nanoclay filled laminate due to exfoliated structure. At 3 wt.% nanoclay filled laminate, about 9%, 21% and 15% increase of strength, modulus and elongation respectively was observed when compared with unfilled laminates.

The outcome of this work provides basic flow characteristics of the nanoclay filled epoxy resin and suggests that designers to select infusion points carefully to produce optimally designed structures during nanoclay filled laminate processing. This result will also be helpful to control the processing parameters during infusion, namely, permeability, V_f, thickness, degree of cure, structure and morphology.

Acknowledgments

The authors gratefully acknowledge the financial support provided by The Claude Leon Foundation of South Africa (Postdoctoral Research Fellowship – 2012/13).

References

[1] Frangopol Dan M, Recek Sébastien. Reliability of fiber-reinforced composite laminate plates. Probab Eng Mech 2003;18(2):119–37.

[2] Fu S-Y, Lauke B, Mäder E, Yue C-Y, Hu X. Tensile properties of short-glass-fiber- and short-carbon-fiber-reinforced polypropylene composites. Compos A Appl Sci Manuf 2000;31(10):1117–25.
[3] Mouzakis Dionysis E, Zoga Helen, Galiotis Costas. Accelerated environmental ageing study of polyester/glass fiber reinforced composites (GFRPCs). Compos B Eng 2008;39(3):467–75.
[4] Bellenger V, Tcharkhtchi A, Castaing Ph. Thermal and mechanical fatigue of a PAgg/glass fibers composite material. Int J Fatigue 2006;28(10):1348–52.
[5] Lee J-Y, Kim T-Y, Kim T-J, Yi C-K, Park J-S, You Y-C, et al. Interfacial bond strength of glass fiber reinforced polymer bars in high-strength concrete. Compos B Eng 2008;39(2):258–70.
[6] Moriwaki Takeshi. Mechanical property enhancement of glass fibre-reinforced polyamide composite made by direct injection moulding progress. Compos A Appl Sci Manuf 1996;27(5):379–84.
[7] Sibold Nathalie, Dufour Christian, Gourbilleau Fabrice, Metzner Marie-Noëlle, Lagrève Christian, Le Pluart Loïc, et al. Montmorillonite clay-polymer nanocomposites: Intercalation of tailored compounds based on succinic anhydride, acid and acid salt derivatives – a review. Appl Clay Sci 2007;38(1–2):130–8.
[8] Sikdar Debashis, Katti Dinesh R, Katti Kalpana S, Bhowmik Rahul. Insight into molecular interactions between constituents in polymer clay nanocomosites. Polymer 2006;47(14):5196–205.
[9] Pavlidou S, Papaspyrides CD. A review on polymer-layered silicate nanocomposites. Prog Polym Sci 2008;38(12):1119–98.
[10] Xidas Panagiotis I, Triantafyllidis Kostas S. Effect on the type of alkylammonium ion clay modifier on the structure and thermal/mechanical properties of glassy and rubbery epoxy-clay nanocomposites. Eur Polym J 2010;46(3):404–17.
[11] Perrin-Sarazin F, Ton-That M-T, Bureau MN, Denault J. Micro- and nano-structure in polypropylene/clay nanocomposites. Polymer 2005;46(25):11624–34.
[12] Paul DR, Robeson LM. Polymer nanotechnology: Nanocomposites. Polymer 2008;49(15):3187–204.
[13] Feng DAI, Ya-hong XU, Ya-ping ZHENG, Xiao-Su YI. Study on morphology and mechanical properties of high-functional epoxy based clay nanocomposites. Chin J Aeronaut 2005;18(3):279–82.
[14] Le Pluart Loïc, Duchet Jannick, Sautereau Henry. Epoxy/montmorillonite nanocomposites: influence of organophilic treatment on reactivity, morphology and fracture properties. Polymer 2005;46(26):12267–78.
[15] Kornmann X, Lindberg H, Berglund LA. Synthesis of epoxy-clay nanocomposites: influence of the nature of the clay on structure. Polymer 2001;42(4):1303–10.
[16] Mohan TP, Ramesh Kumar M, Velmurugan R. Epoxy-clay nanocomposites and hybrids: synthesis and characterization. J Reinf Plast Compos 2009;28(1):17–37.
[17] Mohan TP, Velmurugan R. Rheology and curing characteristics of epoxy-clay nanocomposites. Polym Int 2005;54(10):1653–9.
[18] Lin Li-Yu, Lee Joong-Hee, Hong Chang-Eui, Yoo Gye-Hyoung, Advani Suresh G. Preparation and characterization of layered silicate/glass fiber/epoxy hybrid nanocomposites via vacuum-assisted resin transfer molding (VARTM). Compos Sci Technol 2006;66(13):2116–25.
[19] Chandrasekaran VCS, Advani SG, Santare MH. Influence of resin properties on interlaminar shear strength of glass/epoxy/MWNT hybrid composites. Compos A Appl Sci Manuf 2011;42(8):1007–16.
[20] Brunner AJ, Flüeler P. Prospects in fracture mechanics of "engineering" laminates. Eng Fract Mech 2005;72(6):899–908.
[21] Zhang Jin, Chaisombat Khunlavit, He Shuai, Wang Chun H. Hybrid composite laminate reinforced with glass/carbon woven fabrics for lightweight load bearing structures. Mater Des 2012;36(4):75–80.
[22] Sharma B, Mahajan S, Chhibber R, Mehta R. Glass fiber reinforced polymer-clay nanocomposites: Processing, structure and hygrothermal effects on mechanical properties. Proc Chem 2012;4(2):39–46.
[23] Yuan Xu, Van Hoa Suong. Mechanical properties of carbon fiber reinforced epoxy/clay nanocomposites. Compos Sci Technol 2008;68(3–4):854–61.
[24] Zhou Yuanxin, Pervin Farhana, Rangari Vijaya K, Jeelani Shaik. Influence of montmorillonite clay on the thermal and mechanical properties of conventional carbon fiber reinforced composites. J Mater Process Technol 2007;191(1–3):347–51.
[25] Chandrasekaran VCS, Advani SG, Santare MH. Role of processing on interlaminar shear strength enhancement of epoxy/glass fiber/multi-walled carbon nanotube hybrid composites. Carbon 2010;48(13):3692–9.
[26] Bozkurt Emrah, Kaya Elçin, Tanoğlu Metin. Mechanical and thermal behavior of non-crimp glass fiber reinforced layered clay/epoxy nanocomposites. Compos Sci Technol 2007;67(15–16):3394–403.
[27] Manfredi LB, De Santis H, Vázquez A. Influence of the addition of montmorillonite to the matrix of unidirectional glass fibre/epoxy composites on their mechanical and water absorption properties. Compos A Appl Sci Manuf 2008;39(11):1726–31.
[28] Khan Shafi Ullah, Munir Arshad, Hussain Rizwan, Kim Jang-Kyo. Fatigue damage behaviors of carbon fiber-reinforced epoxy composites containing nanoclay. Compos Sci Technol 2010;70(14):2077–85.
[29] Quaresimin Marino, Salviato Marco, Zappalorto Michele. Fracture and interlaminar properties of clay-modified epoxies and their glass reinforced laminates. Eng Fract Mech 2012;81(3):80–93.
[30] Escola MA, Moina CA, G'omez ACN, Ybarra GO. The determination of the degree of cure in epoxy paints by infrared spectroscopy. Polym Testing 2005;24(5):572–5.
[31] Montserrat S, Roman F, Hutchinson JM, Campos L. Analysis of the cure of epoxy based layered silicate nanocomposites: reaction kinetics and nanostructure development. J Appl Polym Sci 2008;108(2):923–38.
[32] Ton-That MT, Ngo TD, Ding P, Fang G, Cole KC, Hoa SV. Epoxy nanocomposites: analysis and kinetics of cure. Polym Eng Sci 2004;44(6):1132–41.
[33] González-Benito J. The nature of the structural gradient in epoxy curing at a glass fiber/epoxy matrix interface using FTIR imaging. J Colloid Interface Sci 2003;267(2):326–32.
[34] Sánchez-Soto M, Pagés P, Lacorte T, Briceño K, Carrasco F. Curing FTIR study and mechanical characterization of glass bead filled trifunctional epoxy composites. Compos Sci Technol 2007;67(9):1974–85.
[35] Ramadan Adham R, Esawi Amal MK, Gawad Ahmed Abdel. Effect of ball milling on the structure of Na^+-montmorillonite and organo-montmorillonite (Cloisite 30B). Appl Clay Sci 2010;47(3–4):196–202.
[36] Chen Wen-Yi, Wang Yez-Zen, Chang Feng-Chih. Study of curing kinetics and curing mechanism of epoxy resin based on diglycidyl ether of bisphenol A and melamine phosphate. J Appl Polym Sci 2004;92(2):892–900.
[37] Wang Xiaorong, Gillham John K. Tg-Temperature property (TgTP) diagram for thermosetting systems: Anamalous behavior of physical properties vs. extent of cure. J Appl Polym Sci 1993;47(3):425.
[38] Ray Suprakas Sinha, Okamoto Masami. Polymer/layered silicate nanocomposites: a review from preparation to processing. Progr Polym Sci 2003;28(11):1539–641.
[39] Ha SR, Ryu SH, Park SJ, Rhee KY. Effect of clay surface modification and concentration on the tensile performance of clay/epoxy nanocomposites. Mater Sci Eng A 2007;448(1–2):264–8.
[40] Meguid SA, Sun Y. On the tensile and shear strength of nano-reinforced composites interfaces. Mater Des 2004;25(4):289–96.
[41] Chen Bigiong, Evans Julian RG. Impact and tensile energies of fracture in polymer-clay nanocomposites. Polymer 2008;49(23):5113–8.
[42] Bharadwaj RK, Mehrabi AR, Hamilton C, Trujillo C, Murga M, Fan R, et al. Structure-property relationships in cross-linked polyester-clay nanocomposites. Polymer 2002;43(13):3699–705.
[43] Bhanvase BA, Pinjari DV, Gogate PR, Sonawane SH, Pandit AB. Synthesis of exfoliated poly(styrene-co-methyl methacrylate)/montmorillonite nanocomposite using ultrasound assisted *in situ* emulsion copolymerization. Chem Eng J 2012;181–182(1):770–8.
[44] Zaman Izzuddin, Le Quven-Huven, Kuan Hsu-Chiang, Kawashima Nobuyuki, Luong Lee, Gerson Andrea, et al. Interface-tuned epoxy/clay nanocomposites. Polymer 2011;52(2):497–504.
[45] Li Xi, Zhan Zai-Ji, Peng Gui-Rong, Wang Wen-Kui. Nano-disassembling method – A new method for preparing completely exfoliated epoxy/clay nanocomposites. Appl Clay Sci 2012;55(1):168–72.
[46] Mohan TP, Kanny K. Using image analysis for structural and mechanical characterization of nanoclay reinforced polypropylene composites. Engineering 2010;2:802–12.
[47] Product technical data, AMT Composites – South Africa.
[48] Lu HB, Nutt S. Restricted relaxation in polymer nanocomposites near the glass transition. Macromolecules 2003;36(11):4010.
[49] Miyagawa H, Rich MJ, Drzal LT. Amine-cured epoxy/clay nanocomposites. I. Processing and chemical characterization. J Polym Sci Part B Polym Phys 2004;42(23):4384–90.